28

Fault-Tolerant Gait Planning of Multi-Legged Robots

Jung-Min Yang*, Yong-Kuk Park** and Jin-Gon Kim**
*Department of Electrical Engineering, Catholic University of Daegu
**School of Mechanical and Automotive Engineering, Catholic University of Daegu
Republic of Korea

1. Introduction

A fault-tolerant gait of multi-legged systems is defined as a gait which can maintain the gait stability and continue its walking against the occurrence of a leg failure (Yang & Kim, 1998). The notion of the fault-tolerant gait comes from the fact that legged robots with static walking have inherent fault tolerance capability against a failure in a leg, since a failed leg for itself does not cause fatal breakdown or instability to walking motions (Nagy et al., 1994). This means that for a given type of failure, the problem of finding fault-tolerant gaits can be formulated with which legged robots can continue their walking after an occurrence of a failure, maintaining static stability. As a novel field of gait study, fault-tolerant gaits are worth researching since the feature of leg failure can be involved into the frame of gait study and its adverse effect on gait planning can be analyzed with performance criteria such as stability margin, stride length, etc.

Fault-tolerant gaits are classified by the kind of leg failure to be tolerated and the point of time that fault tolerance is carried out, that is, before or after a failure occurs. Several algorithms of fault-tolerant gaits developed in the past can be sorted out by these categories (Chu & Pang, 2002; Lee & Hirose, 2002, Nagy et al, 1994; Yang, 2002). Among them, Yang (Yang, 2002) proposed fault-tolerant gaits for post-failure walking of quadruped robots with a locked joint failure, in which a joint of a leg is locked in a known place (Lewis & Maciejewski, 1997). As one of common failures that can be frequently observed in dynamics of robot manipulators, the locked joint failure reduces the number of degrees of freedom of the robot manipulator by one and consequently its workspace to a certain limit. To establish the fault-tolerance scheme, the reduction of the workspace of a failed leg should be interpreted and reflected based on gait study.

The objective of this article is to develop the fault-tolerant gait algorithm for a locked joint failure when the model of legged robots is *hexapod*. Compared with the previous results on quadruped robots (Yang, 2002, Yang, 2003), the following aspects will be considered in this article for the motion of hexapod robots. First, quadruped robots can have only one gait pattern in static walking, (4→3→4→3⋯), i.e., one leg is lifted off and swung while other three legs are in the support phase. But hexapod robots can have variable gait pattern, i.e., tripod, quadruped and pentaped gaits. In this article, we show that fault tolerance can be realized for walking with any gait and, especially, periodic gaits can be generated using tripod and quadruped gaits for straight-line walking on even terrain. We also present fault-tolerant gaits with non-zero crab angle, or a walking motion with the direction of

Source: Mobile Robots, Moving Intelligence, ISBN: 3-86611-284-X, Edited by Jonas Buchli, pp. 576, ARS/plV, Germany, December 2006

locomotion different from the longitudinal axis of the robot body. Second, the previous result did not take into account kinematic constraints of the failed leg in developing fault-tolerant gait planning. But, there exist singularities in the configuration of a failed leg where legged robots cannot change the present gait due to the failure and are fallen into dead-lock state. We verify that for the existence of fault-tolerant gaits, the configuration of the failed leg must be within a prescribed range of kinematic constraints.

This article is organized as follows: In Section 2, a hexapod prototype is described with conditions on walking mechanism. The configuration of the locked joint failure is also addressed. The kinematic constraints for the existence of fault-tolerant gaits are provided in Section 3. In Section 4, a general scheme for fault-tolerant gait planning is proposed for straight-line walking of a hexapod robot over even terrain. In particular, periodic gaits are derived from the proposed scheme with formulations of the stride length and stability margin. In Section 5, based on the principles of fault-tolerant gait planning for a locked joint failure, periodic crab gaits are proposed in which a hexapod robot has tripod walking after a joint of a leg is locked from failure. In Section 6, a post-failure walking example is addressed in which a hexapod robot walking with the wave gait before a failure could realize fault tolerance by the proposed scheme. Finally, some concluding remarks are given in Section 7.

2. Preliminaries

2.1 Modeling of Hexapod

A two-dimensional model of a hexapod robot is shown in Figure 1. The six legs are placed symmetrically about the longitudinal axis and have rectangular working areas with the length R_x and the width R_y. C_i is the center point of leg i's working area. The robot body is also in the shape of a rectangle with 2U width and distant from working areas by W. C is the center of gravity of the body and the origin of the robot coordinate system X-Y. The crab angle $\alpha(-180^\circ < \alpha \le 180^\circ)$ is defined as the angle between the longitudinal axis of the robot body and the direction of crab walking. α_d, a robot parameter that will be used later in this paper, is defined as the angle between the off-diagonal and the base of the working area.

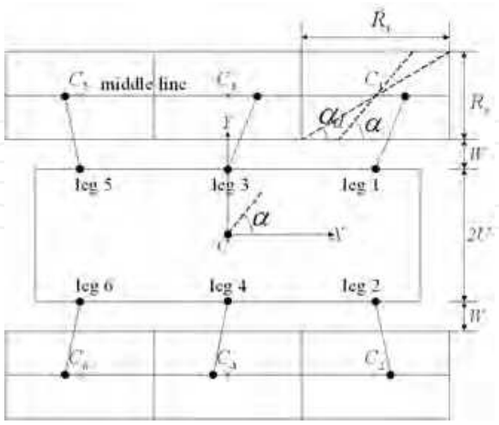

Fig. 1. Two-dimensional model of a hexapod robot.

It is supposed that a leg attached to the hexapod robot has the geometry of the articulated arm (Lewis et al., 1993) shown in Figure 2. This model has two rigid links and three revolute joints; the lower link is connected to the upper link via an active revolute joint and the upper

link is connected to the body via two active revolute joints, one parallel with the knee joint and the other parallel with the body longitudinal axis. Hence the foot point has three degrees of freedom with respect to the body and the overall walking can be driven in any direction. We denote the joint at the main actuator as *joint one*, the joint at the lifting actuator as *joint two,* and the joint at the knee actuator as *joint three*. θ_1, θ_2 and θ_3 are values of each joint angle, and l_1 and l_2 are lengths of the upper and lower links, respectively.

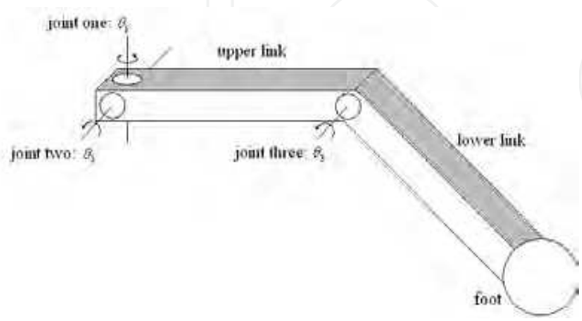

Fig. 2. Three-joint leg model.

By adopting the major premise of gait study (Song & Waldron, 1987), we assume that the robot body remains parallel to the ground, and that the ground is flat over the region affecting the robot workspace. The dimension of the working area of each leg is thus kept the same throughout walking. Moreover, it is assumed that the hexapod robot has static walking in which dynamic effects of legs and the body are negligible. All the mass of the legs is supposed to be lumped into the body and the orientation of the support surface with respect to the gravity vector is irrelevant. Because walking on uneven terrain is precluded in the study, we properly suppose that the hexapod robot has straight-line walking with a regular gait, that is, each leg tracks on the middle line or crab line with angle α of its working area (see Figure 1), paralleled with the trajectory of the center of gravity.

2.2 Review of Locked Joint Failure

A single locked joint failure reduces the number of degrees of freedom in the leg by one and hence inflicts serious damage on mobility of the failed leg (Lewis & Maciejewski, 1997). However, unlike free-swinging failure (Shin & Lee, 1999) and mutilation failure, the locked joint failure does not take away supporting ability from the failed leg. For employing the failed leg in post-failure walking, we should examine the configuration of the failed leg determined by the position of a locked joint and the resulting change of the reachable area.

Figure 3 illustrates the behaviour of a failed leg with the geometry of Figure 2. After joint one of a leg is locked from failure, the kinematics of the failed leg is the same as a two-link revolute joint manipulator. Its workspace is reduced to the plane made of the two links and the reachable region of the foothold position in the working area is projected onto a straight-line of which the lateral view is shown in Figure 3(a). $\hat{\theta}_1$ denotes the locked angle of joint one, and the values of θ_2 and θ_3 are determined by the foothold position. The locked failure at joint two or three yields almost identical post-failure behavior. When joint two or three is locked, the failed leg is tantamount to a one-link manipulator with two revolute joints. Since the altitude of the robot body is assumed to be constant, if one of joints two and three is

locked, the angle of another joint is fixed too for a given foothold position. For instance, joint two is assumed to be locked at $\hat{\theta}_2$ and the failed leg is placed onto the point P in Figure 3(b). Though the leg might have another foothold position P' in kinematics, it is impossible to place onto the point because the altitude of the robot body does not change. Therefore, joint three is also "locked" at $\hat{\theta}_3$ in the configuration of Figure 3(b), and the failed leg moves by swinging joint one as shown in Figure 3(c), making the track of foothold positions in the shape of an arc.

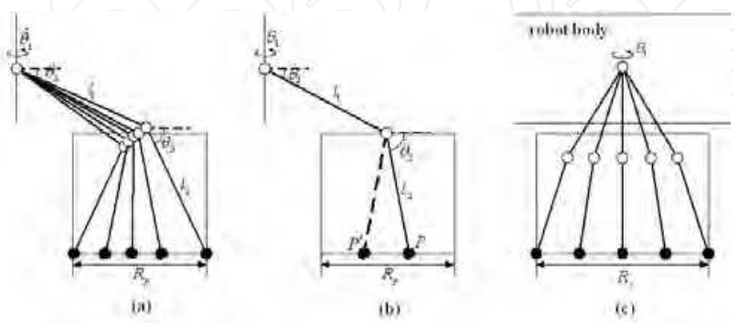

Fig. 3. Locked joint failure: (a) lateral view of the locked failure at joint 1, (b) lateral view of the locked failure at joint 2 (or joint 3) and (c) front view of the locked failure at joint 2 (or joint 3).

3. Kinematic Constraints

While the previous study investigated constrained motions of a failed leg in detail, it did not take into account kinematic constraints necessary for the existence of fault-tolerant gaits. In this section, we show that there is a range of kinematic constraints which the configuration of a failed leg should satisfy for guaranteeing the existence of fault-tolerant gaits.

3.1 Straight-line motion

3.1.1 Failure of joint one

In the first, let us consider the case where joint one is locked from failure. The failed leg in this case cannot take longitudinal swing with respect to the body and can take only lateral swing using the remaining normal joints as shown in Figure 4(a), where $\hat{\theta}_1$ is the locked angle of joint one. The motion of such a leg becomes that of a two-link revolute-joint manipulator. Its workspace is reduced to the plane made of the links and the reachable region of the foothold position in the working area is projected onto a straight-line shown in Figure 4(b). The failed leg can place its foot on the one and only foothold position, denoted by P, the intersection point of the foot trajectory (middle line of the working area) and the reachable line. For such an intersection point to exist, locked angle $\hat{\theta}_1$ must be in the range of

$$\hat{\theta}_{1,\min} \le \hat{\theta}_1 \le \hat{\theta}_{1,\max}$$

as shown in Figure 4(b), where all the angles are measured from the bisecting line of the working area in the clockwise direction. $\hat{\theta}_{1,\min}$ and $\hat{\theta}_{1,\max}$ are calculated as

$$\hat{\theta}_{1,\min} = -\arctan\left(\frac{R_x}{R_y + 2W}\right)$$

$$\hat{\theta}_{1,\max} = \arctan\left(\frac{R_x}{R_y + 2W}\right)$$

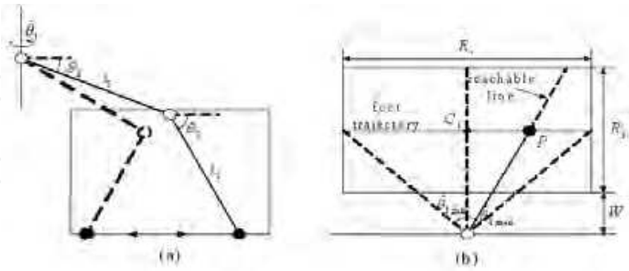

Fig. 4. Locked failure at joint one in straight-line walking: (a) lateral view and (b) kinematic constraint.

3.1.2 Failure of joint two

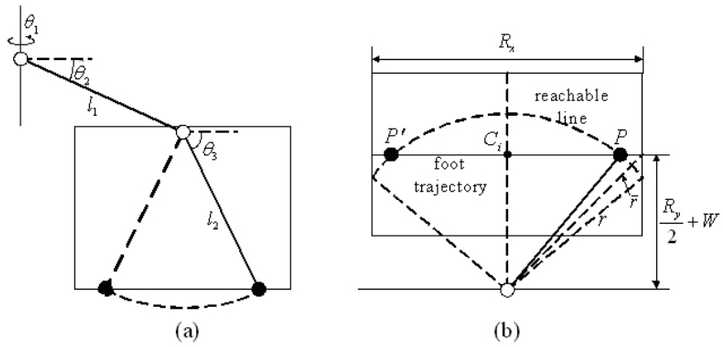

Fig. 5. Locked failure at joint two in straight-line walking: (a) lateral view and (b) kinematic constraint.

When joint two is locked from failure, the failed leg can move only the lower link by joint three for vertical swing. Depending on the configuration at the moment of failure, the failed leg can be placed on the inner foothold position or the outer position as shown in Figure 5(a). The resulting reachable region on the working area is thus projected onto a line of arc shape shown in Figure 5(b). Unlike the case of joint one where there is only one foothold position, the failed leg in this case can place its foot on one of two possible foothold positions, *P* and *P'*, in the foot trajectory. The kinematic constraint for guaranteeing such foothold positions can be described as

$$\frac{R_y}{2} + W \le r \le \bar{r} \tag{1}$$

where *r* is the radius of the arc and $\bar{r}$ is the distance between the leg attachment point and the front-end(or rear-end) position projected onto the *X*-*Y* plane. If the radius of the arc *r* is in the above range, there exists at least one intersection point of the arc and the foot trajectory. For describing (1) in terms of joint angles and robot parameters, let us rewrite $\bar{r}$ and *r* as

$$\bar{r} = \frac{1}{2}\sqrt{R_x^2 + (R_y + 2W)^2}$$
$$r = l_1 \cos\hat{\theta}_2 + l_2 \cos\theta_3 \tag{2}$$

where $\hat{\theta}_2$ is the locked angle of joint two. Note that r is identical to the length of the leg projection onto the working area. Since the robot body is supposed to have a constant altitude, the angle of joint three θ_3 should also be fixed in failure mode (see Figure 5(a)). Substituting (2) into (1) leads to

$$\frac{R_y}{2} + W \le l_1 \cos\hat{\theta}_2 + l_2 \cos\theta_3 \le \frac{1}{2}\sqrt{R_x^2 + (R_y + 2W)^2}$$

The above result prescribes the kinematic constraint of locked angle $\hat{\theta}_2$ which guarantees the existence of the fault-tolerant gait for straight-line walking.

Consider the case of a locked failure at joint three as a remark. The constrained motion of the failed leg is almost identical to the case of joint two. If joint three is locked from failure, the leg is reduced to a one-link manipulator with two revolute joints (Craig, 2003), and the restricted reachable region projected onto the working area is of arc shape too. Therefore, the kinematic constraint for the existence of the fault-tolerant gait is the same as the case of joint two:

$$\frac{R_y}{2} + W \le l_1 \cos\theta_2 + l_2 \cos\hat{\theta}_3 \le \frac{1}{2}\sqrt{R_x^2 + (R_y + 2W)^2}$$

where $\hat{\theta}_3$ is the locked angle of joint three.

3.2 Crab Walking

In crab walking, the damage caused by a locked joint failure turns out to be the reduction of the range of the crab angle that the hexapod can have after a failure (Yang, 2003). We investigate such kinematic constraints for a given configuration of a locked failure.

3.2.1 Failure of joint one

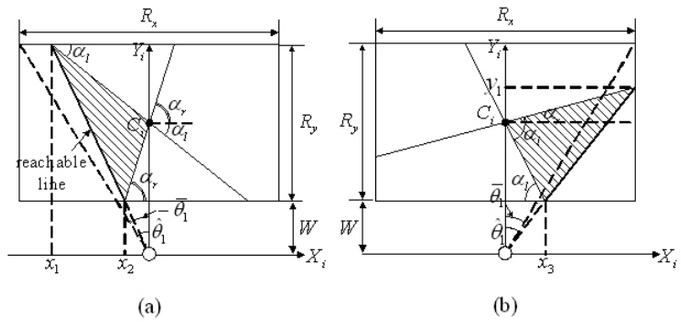

Fig. 6. Kinematic constraint for the locked failure in crab walking at joint one: (a) $|\hat{\theta}_1| < |\bar{\theta}_1|$ and (b) $|\hat{\theta}_1| \ge |\bar{\theta}_1|$.

Figure 6 illustrates the kinematic constraint for fault-tolerant crab gaits when joint one of a leg is locked at $\hat{\theta}_1$. For clarity's sake, we assume that leg i's coordinate system $X_i - Y_i$ is

located at the leg attachment point and the angle of joint one is measured from the bisecting line of the working area (the Y_i axis) in the clockwise direction, whereas the crab angle is measured from the X axis of the robot coordinate system in the counterclockwise direction (see Figure 1). As was illustrated in Figure 3, the reachable region of the foothold position is projected onto a straight-line in the working area. For the hexapod robot to be able to have crab walking after a failure, the foot trajectory must intersect the reachable line, in which the intersection point is to be the foothold position of the failed leg throughout post-failure walking. Therefore, the crab angle α should be within the shaded areas depicted in Figure 6 and should satisfy the following kinematic constraint:

$$\alpha_l \le \alpha \le \alpha_r \tag{3}$$

where α_l and α_r are the leftmost and rightmost limits, respectively. Since the working area is of rectangular shape, α_l and α_r are expressed differently according to the relative values of $\bar{\theta}_1$ and $\hat{\theta}_1$, where $\bar{\theta}_1$ is the locked angle of joint one that makes the reachable line cross the upper corner of the working area.

i) $\left|\hat{\theta}_1\right| < \left|\bar{\theta}_1\right|$

If the locked angle is in the above range, the reachable line ends at the upper boundary of the working area. Referring to Figure 6(a), α_l is described as

$$\alpha_l = -\arctan\left(\frac{R_y}{2x_1}\right)$$

x_1, the end position of the reachable line on the upper boundary of the working area, is calculated as $x_1 = (R_y + W)\tan\hat{\theta}_1$. Hence α_l can represented by the robot parameters as

$$\alpha_l = -\arctan\left(\frac{R_y}{2(R_y + W)\tan\hat{\theta}_1}\right) \tag{4}$$

Likewise, α_r is calculated as

$$\alpha_r = \arctan\left(\frac{R_y}{2x_2}\right) = \arctan\left(\frac{R_y}{2W\tan\hat{\theta}_1}\right) \tag{5}$$

It should be noted from Figure 6(a) that both equations (4) and (5) are obtained for the case of $-\bar{\theta}_1 < \hat{\theta}_1 < 0$. But, the case of $0 < \hat{\theta}_1 < \bar{\theta}_1$ is symmetric with respect to the former case and its kinematic constraint can be easily resolved as below:

$$\alpha_l = -\arctan\left(\frac{R_y}{2W\tan\hat{\theta}_1}\right) \qquad \left(0 < \hat{\theta}_1 < \bar{\theta}_1\right)$$

$$\alpha_r = \arctan\left(\frac{R_y}{2(R_y + W)\tan\hat{\theta}_1}\right)$$

ii) $\left|\hat{\theta}_1\right| \ge \left|\bar{\theta}_1\right|$

The reachable line of the failed leg with a locked angle in the above range ends at the side boundary of the working area. From Figure 6(b), the values of α_l and α_r are described as

$$\alpha_l = -\arctan\left(\frac{R_y}{2x_3}\right)$$
$$\alpha_r = \arctan\left(\frac{y_1 - (R_y/2 + W)}{R_x/2}\right)$$

Since x_3 and y_1 are obtained from trigonometry as $x_3 = W\tan\hat{\theta}_1$ and $y_{1=(R_x/2)\tan\hat{\theta}_1}$, α_l and α_r are reduced to

$$\alpha_l = -\arctan\left(\frac{R_y}{2W\tan\hat{\theta}_1}\right) \qquad (\hat{\theta}_1 \geq \overline{\theta}_1)$$
$$\alpha_r = \arctan\left(\frac{R_x - (R_y + 2W)\tan\hat{\theta}_1}{R_x\tan\hat{\theta}_1}\right)$$

Like the former case, the values of α_l and α_r for the case of $\hat{\theta}_1 \leq -\overline{\theta}_1$ can be obtained by symmetry:

$$\alpha_l = -\arctan\left(\frac{R_x - (R_y + 2W)\tan\hat{\theta}_1}{R_x\tan\hat{\theta}_1}\right)(\hat{\theta}_1 \leq -\overline{\theta}_1)$$
$$\alpha_r = \arctan\left(\frac{R_y}{2W\tan\hat{\theta}_1}\right)$$

3.2.2 Failure of joint two

Figure 7 illustrates the kinematic constraint for fault-tolerant crab gaits when joint two of a leg is locked. Because a locked failure at joint three yields the same kinematic characteristics as that of joint two, its analysis is omitted in this paper. As shown in the figure, the reachable region of the foothold position becomes an arc with the radius *r*. The kinematic constraint is determined according to the length of *r*.

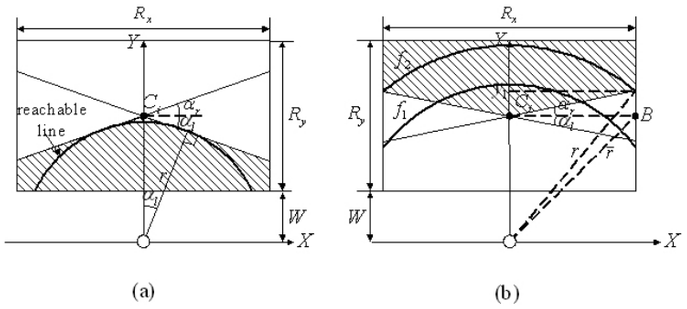

Fig. 7. Kinematic constraint for the locked failure in crab walking at joint two: (a) $r < R_y/2 + W$ and (b) $r \geq R_y/2 + W$.

i) $r < R_y/2 + W$

If *r* is in the above range, the reachable arc cannot enclose the center point C_i of the working area. Hence, for the foot trajectory to intersect the arc, the crab angle should be within the shaded area marked in Figure 7(a). The kinematic constraint for the crab angle α is thus

$$\alpha_r \le \alpha \le \alpha_l \tag{6}$$

From Figure 7(a), α_l is obtained as

$$\alpha_l = -\arccos\left(\frac{r}{R_y/2+W}\right)$$

Since *r* is the length of the leg projection onto the working area,

$$r = l_1\cos\hat{\theta}_2 + l_2\cos\hat{\theta}_3$$

where $\hat{\theta}_2$ is the locked angle of joint two and $\hat{\theta}_3$ is the corresponding fixed angle of joint three (refer to Figure 3). Applying the above equation, α_l is re-written as

$$\alpha_l = -\arccos\left(\frac{l_1\cos\hat{\theta}_2 + l_2\cos\hat{\theta}_3}{R_y/2+W}\right) \tag{7}$$

As the reachable arc is symmetric with respect to the Y_i axis of the working area, α_r is equal to $-\alpha_l$:

$$\alpha_r = \arccos\left(\frac{l_1\cos\hat{\theta}_2 + l_2\cos\hat{\theta}_3}{R_y/2+W}\right) \tag{8}$$

Substituting (7) and (8) into (6) completes the kinematic condition for the crab angle in the case of $r < R_y/2+W$.

ii) $R_y/2+W \le r < \bar{r}$

In Figure 7(b), $\bar{r}$ denotes the distance between the leg attachment point and the point *B*, the middle point of the right boundary of the working area. The case of $R_y/2+W \le r < \bar{r}$ is observed most commonly in the failure situation, where the hexapod robot can walk with any crab angle since there exists always the intersection point between the reachable arc and the foot trajectory. f_1 in Figure 7(b) is an example of such a reachable arc which lies in this range.

iii) $\bar{r} \le r$

If *r* is greater than or equal to $\bar{r}$, the reachable arc is drawn, for example, like f_2 in Figure 7(b). Thus the foot trajectory guaranteeing the existence of the fault-tolerant crab gait should be in the shaded area in Figure 7(b) and its kinematic constraint is expressed the same as (6). α_r is found from Figure 7() to be

$$\alpha_r = \arctan\left(\frac{y_1 - (R_y/2+W)}{R_x/2}\right) \tag{9}$$

where is reduced to

$$y_1 = \sqrt{r^2 - (R_x/2)^2} = \sqrt{(l_1\cos\hat{\theta}_2 + l_2\cos\hat{\theta}_3)^2 - (R_x/2)^2} \tag{10}$$

Like the former case, α_l is equal to α_r except the minus sign. Hence, from (9) and (10), we have

$$\alpha_l = -\arctan\left(\frac{\sqrt{4(l_1\cos\hat{\theta}_2 + l_2\cos\hat{\theta}_3)^2 - R_x^2} - (R_y/2 + W)}{R_x}\right)\left(\bar{r} \le r\right)$$

$$\alpha_r = \arctan\left(\frac{\sqrt{4(l_1\cos\hat{\theta}_2 + l_2\cos\hat{\theta}_3)^2 - R_x^2} - (R_y/2 + W)}{R_x}\right)$$

4. Fault-Tolerant Gaits: Straight-Line Motion

4.1 General Scheme

In the previous research, we have described constrained motions of a leg when a locked joint failure occurs to each of the three joints, respectively, and proposed the following principles of fault-tolerant gait planning:

Principles of Fault-Tolerant Gait Planning for a Locked Joint Failure (Yang, 2002)

a) When the failed leg is in the support phase, the robot body does not translate because the failed leg cannot maintain the current foothold position.
b) When the failed leg is in the transfer phase, it does not have active swing with respect to the body motion and is moved only passively by the translation of the body.

Let us examine the meaning of the above principles. When the robot body translates in legged locomotion, the configurations of all the supporting legs should be simultaneously changed to maintain the current foothold positions. If a locked failure occurs to a joint of a leg, however, the rank of Jacobian of the failed leg is reduced by one (Roberts & Maciejewski, 1996) and there exists no solution space of the inverse kinematics with which the foothold position of the failed leg remains the same against the translation of the body. Thus, the robot body should not translate when the failed leg is in the support phase (Principle a). Furthermore, the forward movement of a leg with respect to the robot body is inexecutable with a locked joint. For instance, if joint one of a leg is locked from failure, the failed leg cannot take active swing with respect to the robot body (see Figure 3(a)). On the other hand, if joint two or three is locked from failure, the accessible area where the failed leg could place its foot is reduced to only a partial region of the working area (see Figure 3(b) and (c)), which forbids normal straight-line walking with continuous leg swing. Therefore, it is prescribed that the failed leg is moved only passively by the translation of the body (Principle b).

4.2 Periodic Walking

In terms of mobility, it would be more advantageous that the robot walking with a periodic gait before a failure could preserve its periodicity (with a different gait pattern) even after a fault event. Based on the principles of fault-tolerant gait planning, we propose fault-tolerant periodic gaits for hexapod robots. Among the periodic gaits hexapod robots can have in static walking, quadruped gaits and tripod gaits are proposed in this section. The generation procedure of pentaped gaits, in which five legs are always in the support phase during walking, is similar to the other cases and omitted.

4.2.1 Quadruped gait

In quadruped gaits, two legs are always in the transfer phase. Figure 8 shows the algorithm of the fault-tolerant quadruped gait. Since a pair of legs is simultaneously lifted off and placed, the quadruped gait resulting from the algorithm belongs to a singular gait. Provided

that there is no timing gap between movements of two pairs of legs, the number of supporting legs always remains four. There are three movements of a pair of legs during the cycle time and the robot body advances only after a failed leg is lifted off. According to the principles of fault-tolerant gait planning, the final pair of leg in the transfer phase, including a failed leg, does not take active swing while the robot body moves.

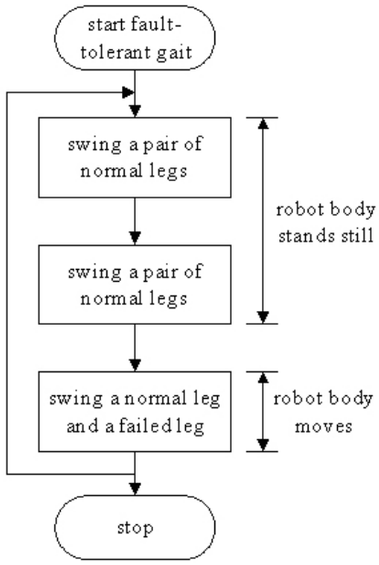

Fig. 8. Algorithm of the fault-tolerant qaudruped gait.

Let us determine the leg sequence and the stride length formula based on the algorithm in Figure 8. The leg sequence with which a quadruped gait can have the maximum longitudinal stability margin (Song & Waldron, 1987) in straight-line walking is known to be (2,5)-(3,4)-(1,6) when the hexapod robot has the prototype shown in Figure 1 (Yang, 1999). In other words, lifting two legs in the symmetric positions with respect to the center of gravity guarantees the maximum stability to the resulting support pattern. The leg stroke, the distance through which the foot is translated relative to the body during the support phase (Song & Waldron, 1987), should be equal to the stride length if the gait is periodical. Therefore, if the stride length of the robot body is chosen, the leg stroke is determined equally.

Figure 9 illustrates the proposed quadruped gait with stride length λ for a locked joint failure at leg 1. Quadruped gaits for a failure at other legs can be derived by symmetry of the hexapod. Black circles denote foothold positions of supporting legs and white circles denote the previous locations of foothold positions. Dash-dotted rectangles are support patterns obtained from lifting two legs. Without loss of generality, the periodic gait sequence is supposed to start with all the six legs set to be in the support phase on the foothold positions in Figure 9(a), where normal legs are placed $_{(R_x-\lambda)/2}$ in front of their rear-end positions and the failed leg lands on a point with distance $x_{1\ (0\le x_1\le R_x)}$ from its rear-end position. Leg 2 and leg 5 are lifted off in the first and moved as much as λ in the $+X$ direction (Figure 9(b)). Next, leg 3 and leg 4 are lifted off and moved the same distance (Figure 9(c)). Because leg 1 is in the support phase, the robot body should not move in these states. The fault tolerance is realized in Figure 9(d) where leg 1 is lifted off with leg 6 and is transferred forward by the movement of the robot body. It is noted that working areas of the initial state are drawn fixed in Figure 9(d) for the convenience of illustration. In fact, the real locations of

the areas change as the body moves. By closing the behavior in Figure 9(d), one period of the leg sequence is accomplished. The longitudinal stability margin of this gait sequence is determined by the shortest of S_{25} and S_{16}, which are the longitudinal stability margins of the states obtained from lifting (leg 2, leg 5) and (leg 1, leg 6), respectively (see Figure 9(b) and (d)). S_{25} and S_{16} are calculated as

$$S_{25} = \frac{1}{4}(2x_1 + R_x - \lambda)$$

$$S_{16} = \frac{1}{2}(R_x - \lambda)$$

Therefore, longitudinal stability margin $S(\lambda)$ of the quadruped gait with stride length λ is derived as

$$S(\lambda) = \min\left[\frac{1}{4}(2x_1 + R_x - \lambda), \frac{1}{2}(R_x - \lambda)\right]$$

Restating the above equation according to the range of x_1 leads to

$$S(\lambda) = \begin{cases} (2x_1 + R_x - \lambda)/4, & x_1 < (R_x - \lambda)/2 \\ (R_x - \lambda)/2, & x_1 \geq (R_x - \lambda)/2 \end{cases} \tag{11}$$

This result implies that the stability of the fault-tolerant quadruped gait increases as the foothold position of the failed leg is more distant from the rear-end position in its working area. Because the failed leg cannot have active swing, the longest stroke which can be obtained in fault-tolerant periodic gaits is equal to R_x, the length of the working area (Yang, 2002). Thus the range of the stride length should be $0 < \lambda \leq R_x$. If λ is equal to R_x, $S(\lambda)$ becomes zero from (11). This complies with a corollary in gait study that a periodic gait with its maximum stride length has the marginal stability margin.

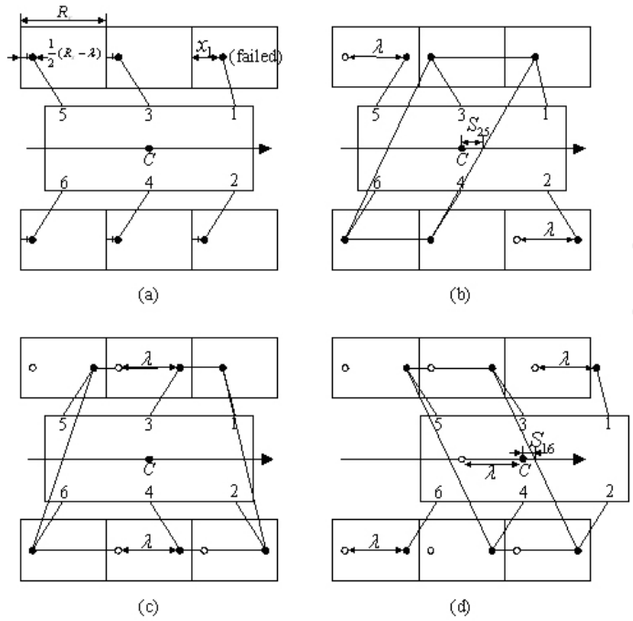

Fig. 9. The periodic quadruped gait for a locked failure at leg 1: (a) initial state, (b) swing leg 2 and leg 5, (c)swing leg 3 and leg 4, and (d) swing leg 1 and leg 6 with the body movement.

4.2.2 Tripod gait

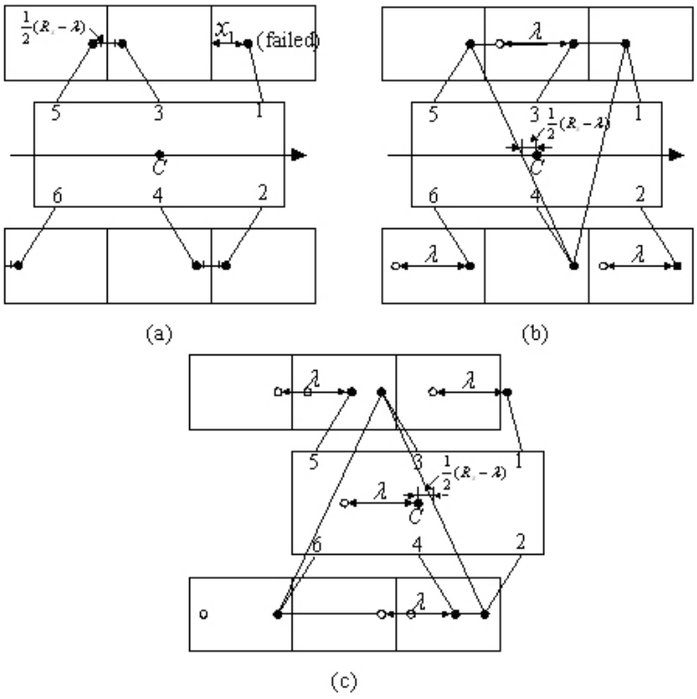

Fig. 10. The periodic tripod gait for a locked failure at leg 1: (a) initial state, (b) swing legs 2, 3 and 6, and (c) swing legs 1, 4 and 5 with the body movement.

The tripod gait has been adopted as the standard gait for hexapod robots (Miao & Howard, 2000) and is regarded as the fastest gait with the minimum stability. Figure 10 shows the tripod gait with stride length λ for a locked joint failure at leg 1. Like the quadruped gait, all the legs are supposed to be in the support phase with the foothold positions given in Figure 10(a). The leg sequence is (2, 3, 6)-(1, 4, 5), the same as that of the standard tripod gait on even terrain (Lee et. al, 1988), but, from the principles of fault-tolerant gait planning, the robot body has discontinuous movement.

The stability margin of the tripod gait is determined only by the stride length, regardless of the foothold position of the failed leg. This is because when the failed leg (leg 1) is in the support phase, the boundary of the support pattern made of the two normal legs (leg 4 and leg 5) has always the shortest distance from the vertical projection of the center of gravity (Figure 10(b)). Referring to Figure 10(b) and (c), the longitudinal stability margin is derived as

$$S(\lambda) = \frac{1}{2}\left(R_x - \lambda\right) \tag{12}$$

5. Fault-Tolerant Gaits: Crab Walking

Based on the general algorithm of fault tolerance for straight-line motion, the fault-tolerant periodic crab gait is proposed in this section. For the sake of simplicity, only the procedure of tripod crab gaits is addressed while the quadruped crab gait is omitted.

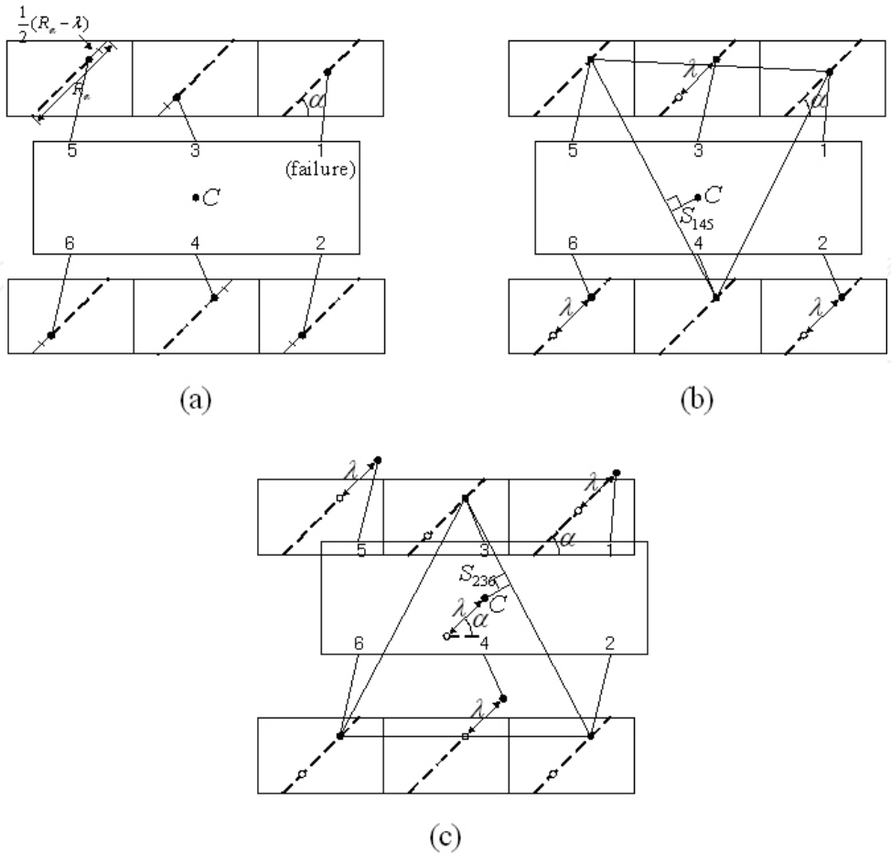

Fig. 11. Fault-tolerant periodic crab gait: (a) initial state, (b) swing legs 2, 3 and 6 and (c) swing legs 1, 4 and 5 with body moving.

Figure 11 shows the proposed fault-tolerant tripod crab gait where a locked joint failure occurs to leg 1. Tripod crab gaits for a failure at other legs can be derived by symmetry of the hexapod. It is noted that the crab angle α should satisfy the kinematic constraints derived in the previous section. Figure 11(a) is the initial state. Legs 2, 3 and 6, the tripod consisting of normal legs, are placed $(R_\alpha - \lambda)/2$ in front of their rear boundaries along the foot trajectory, where R_α is the length of the foot trajectory with the crab angle α with the following value:

$$R_\alpha = \begin{cases} R_y / \sin\alpha & \alpha_d < \alpha \le 90^\circ \\ R_y / \cos\alpha & 0 \le \alpha \le \alpha_d \end{cases}$$

Because the failed leg does not have active swing, the stride length λ cannot be greater than R_α and lies in the range of $0 < \lambda \le R_\alpha$. Leg 4 and leg 5, the two normal legs of another tripod, are placed $(R_\alpha - \lambda)/2$ behind their front boundaries along the foot trajectory in the initial state, and leg 1, the failed leg, is on the foothold position given by the failure configuration (see Figures 6 and 7). According to the leg sequence of the standard tripod gait, the tripod (2, 3, 6) is lifted off first in Figure 11(b) and moved as much as λ, while the robot body stands still. Then, another tripod (1, 4, 5) is lifted off and moved passively

with the translation of the body by λ in Figure 11(c), which completes one cycle of the gait. Dash-dotted triangles in Figure 11(b) and (c) are support patterns obtained when a tripod is in the transfer phase. Since the gait stability of a periodic gait is defined as the minimum value of the stability margin in one cycle, the gait stability of the crab gait with the crab angle α and stride length λ, denoted by $S(\alpha, \lambda)$, is determined as the shortest of s_{145} (Figure 11(b)) and s_{236} (Figure 11(c)). But s_{145} and s_{236} are found to be the same value and are derived as the following:

$$S(\alpha,\lambda)=\left(\frac{R_x}{2}-\frac{\lambda}{2}\left(\cos\alpha+\frac{R_x}{R_x+2W+2U}\sin\alpha\right)\right)\frac{R_y+2W+2U}{\sqrt{(R_y+2W+2U)^2+R_x^2}} \tag{13}$$

If $\alpha=0^\circ$ and the gait has the longest stride length, i.e., $\lambda=R_0=R_x$, then $S(0^\circ,R_x)=0$ in the above equation. This result coincides with that of the fault-tolerant tripod gait with straight-line motion (refer to Eq. (12)). Also, note that $S(\alpha, \lambda)$ is always a positive value if $\alpha>0^\circ$. This means that the fault-tolerant crab gait is advantageous over the straight-line motion in terms of the gait stability.

If there is no time lag between the states of Figure 11(a) ~ (c), the fault-tolerant crab gait has duty factor 1/2, the same as the gait with straight-line motion. This implies that the hexapod robot maintains its mobility as much as the straight-line motion against a locked failure even though it walks with a non-zero crab angle. In addition, the gait stability (13) is irrelevant to the foothold position of the failed leg. Hence the proposed crab gait promises successful post-failure walking for any locked failure.

6. Post-Failure Walking Example

In most cases, a gait of the hexapod robot at the moment of a locked failure may not belong to any state of the proposed periodic gaits. To change the present gait into a state of the proposed periodic gaits, some pre-adjustment of the leg position and the body movement are necessary. This issue will be discussed as a case study in this section.

6.1 Normal Walking: Wave Gait

In this section, the proposed gait planning is applied to a post-failure walking problem of a hexapod robot. We assume that the hexapod robot has been moving with the wave gait and duty factor β =2/3 before a locked joint failure occurs to leg 1. The wave gait is a standard periodic gait of straight-line motion and mostly well known in the area of level-going (Song & Choi, 1990). Its behavior can be analyzed using the gait diagram and the stationary gait pattern. Figures 12 and 13 are the gait diagram and the stationary gait pattern of the wave gait with β =2/3, respectively. A darkened solid line in Figure 12 represents the support phase of a leg and is cast on the leg stroke in the stationary gait pattern in Figure 13. Each leg stroke is then divided into equal segments labeled according to the times of the corresponding argument in the gait diagram. The support pattern at any instant of time can be easily constructed by just connecting all the segments with the same label. For example, the support pattern immediately after leg 1 is lifted off can be obtained by connecting all the segments with label 4, except that of leg 2, since leg 2 has been already lifted. The support pattern is thus the dash-dotted rectangle in Figure 13.

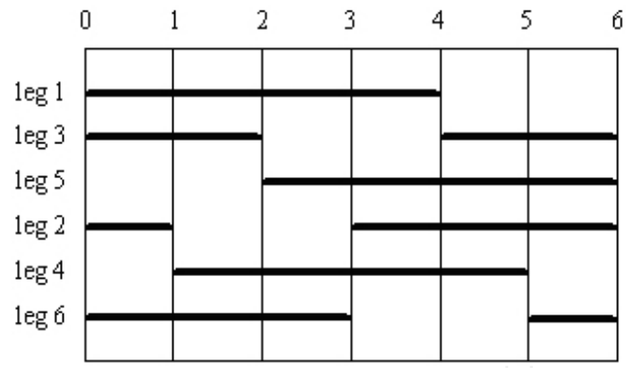

Fig. 12. Gait diagram of the wave gait with β =2/3.

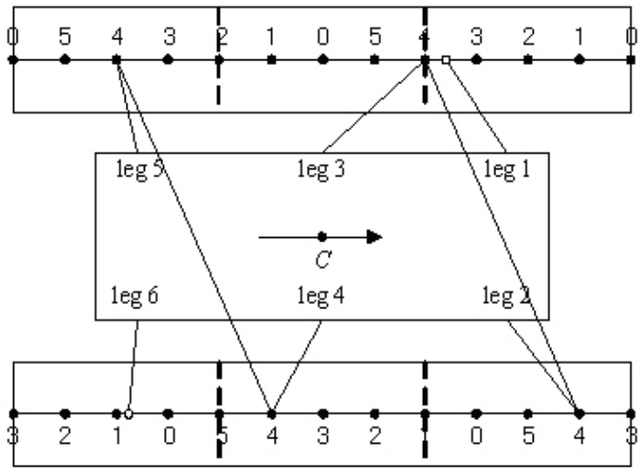

Fig. 13. The stationary gait pattern.

6.2 Post-Failure Walking

We investigate the adjustment procedure for the two cases, where the failed leg is in the support phase and the transfer phase at the moment of a locked joint failure, respectively. Let us denote T as the cycle time and $t_f (0 \le t_f < T)$ as the time by which the occurrence of a locked joint failure in leg 1 lags behind the contact of leg 1 on the ground. Since the wave gait with β =2/3 is a type of quadruped gaits, we demand that post-failure walking should also be a quadruped gait. For the simplicity of analysis, it is assumed that the fault-tolerant gait in post-failure walking has the maximum stride length. Note that when $\lambda = R_x$, all the normal legs in the fault-tolerant quadruped gait are lifted off at the rear-end positions and placed on the front-end positions in one period (refer to Figure 9).

6.2.1 Failure in the support phase

If leg 1 fails in the support phase, t_f is in the range of $0 \le t_f \le 2T/3$. As two legs are always in the transfer phase, the gait transition procedure is made by the following steps:

i) The robot body halts the movement at the instance of failure.

ii) If leg 6 is in the transfer phase, it is placed on the rear-end position of its working area. Other legs in the transfer phase are placed on their front-end positions.
iii) Find a state of the fault-tolerant quadruped gait to which the present state can be transformed with the minimum number of the change of the foothold positions, and complete the gait transition.

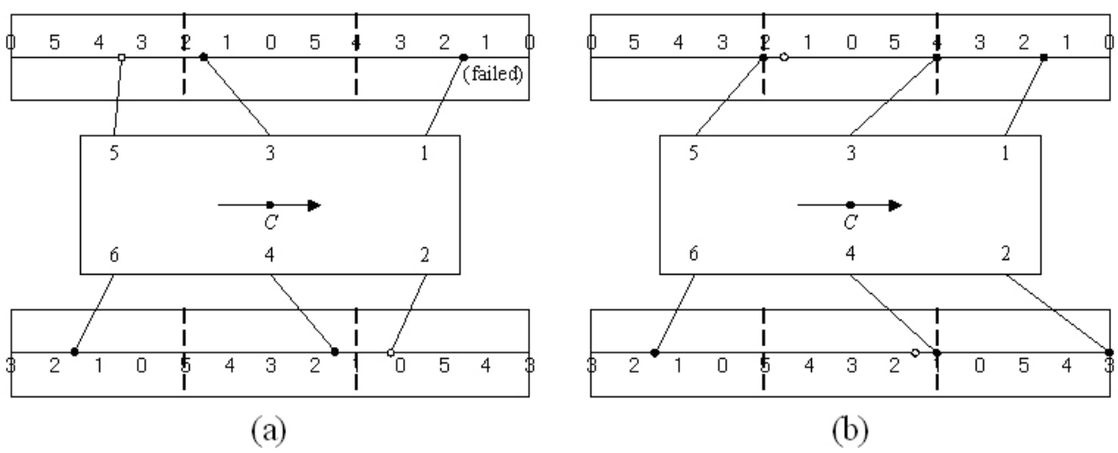

Fig. 14. Gait transition procedure when $T/6 < t_f < T/3$: (a) the state at the instance of failure, (b) place leg 2 and leg 5 and swing leg 3 and leg 4.

Recall that leg 1, the failed leg, is moved passively with leg 6 in the final state of the fault-tolerant quadruped gait in Figure 9. Thus if leg 6 is in the transfer phase, it should be placed on the rear-end position for the lift-off with leg 1. Other normal legs in the transfer phase should be placed on their front-end positions for minimizing required adjustments of the foothold position before starting fault-tolerant walking.
As a specific example of applying the above transition steps, let us assume that leg 1 fails in the range of $T/6 < t_f < T/3$. Figure 14 shows the gait transition procedure for this case. Leg 2 and leg 5, the two transferring legs at the moment of failure, are placed on their front-end positions in the first, followed by the swing of leg 3 and leg 4. The resulting state in Figure 14(b) is tantamount to the state where the failed leg is about to be lifted in the fault-tolerant periodic gait, i.e., Figure 9(c). By lifting leg 1 and leg 6 and moving the robot body after the state of Figure 9(b), the fault-tolerant quadruped gait can be initiated.

6.2.2 Failure in the transfer phase

If leg 1 fails in the transfer phase, t_f is in the range of $2T/3 \le t_f < T$. In a similar manner to the case of the support phase, the robot body halts its movement at the moment of failure and two legs in the transfer phase find competent foothold positions. For example, the gait transition procedure when t_f is in the range of $2T/3 < t_f < 5T/6$ is illustrated by Figure 15. Since leg 1 and leg 6 are in the transfer phase, the initial state is like Figure 15(a). Figure 15(b) shows the placement of the transferring legs. Leg 1, the failed leg, should be placed on a restricted position and leg 6 is placed on its rear-end position to be lifted off with leg 1

after the transition procedure. The foothold positions of the remaining normal legs are adjusted in Figure 15(c) and the hexapod is ready to start the fault-tolerant periodic gait. Note that both the transition procedures in Figures 14 and 15 are dead-lock free and guaranteed for any value of λ. They are also efficiently made in that the number of the change of the foothold positions is minimized.

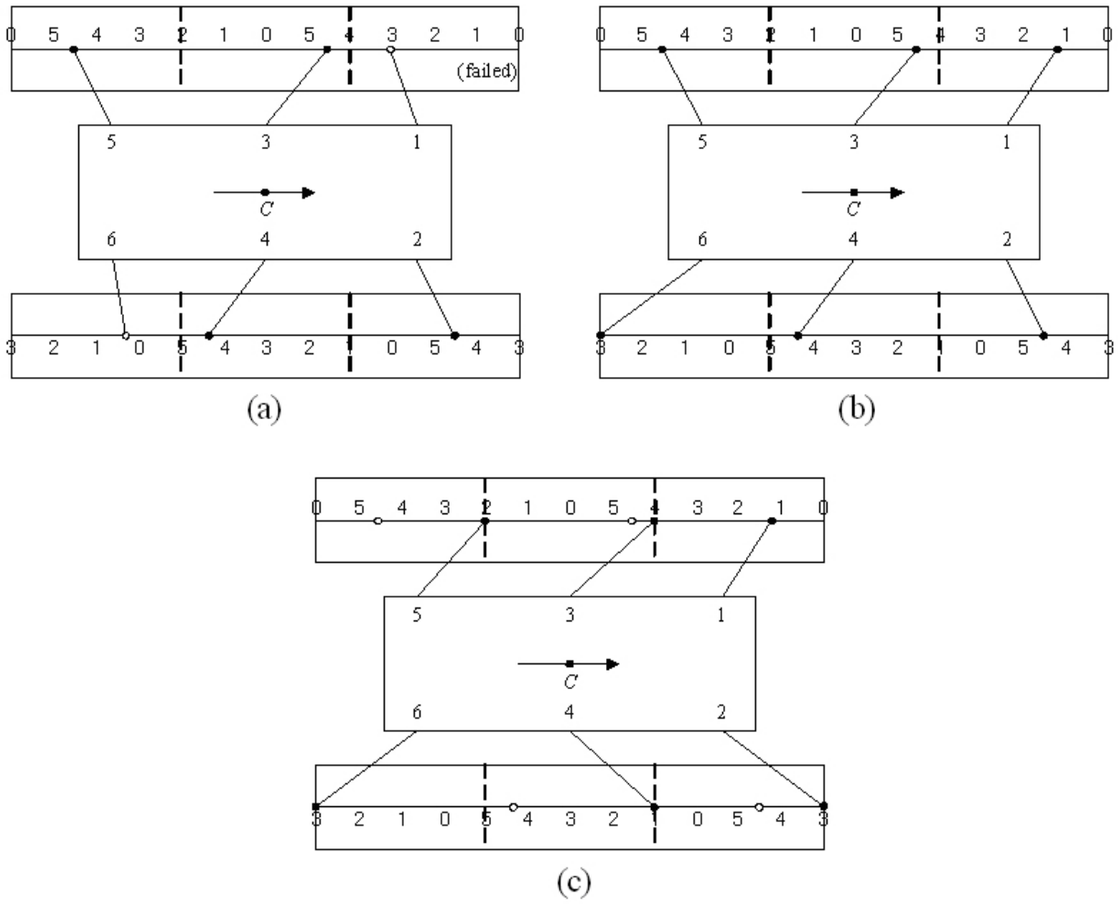

Fig. 15. Gait transition procedure when $2T/3 < t_f < 5T/6$: (a) the state at the instance of failure, (b) place leg 1 and leg 6, and (c) swing (leg 2, leg 5) and (leg 3, leg 4).

6.3 Comparison of Gait Performance

Let us examine the change of gait performance caused by the transition to the fault-tolerant gait. Figure 16 is the gait diagram of the proposed fault-tolerant quadruped gait in Figure 9. For a clear comparison, we assume that there is no resting stage between the placement of a pair of legs and the lift-off of another pair in the quadruped gait. From the gait diagram, the duty factor is obtained as 2/3, the same as that of the wave gait. But the stride length of the fault-tolerant quadruped gait is R_x, less than $3R_x/2$ of the wave gait with β =2/3 (Song & Choi, 1990). Therefore, it can be said that the proposed fault-tolerant gait has no loss of the duty factor against a locked joint failure and its performance is degenerated only in the stride length, which is an inevitable adverse effect of the locked joint failure.

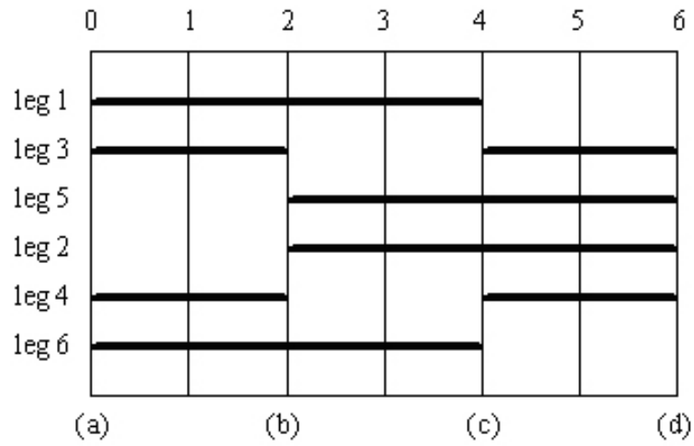

Fig. 16. Gait diagram of the fault-tolerant gait with straight-line motion.

7. Conclusion

In this article, gait planning for static walking of hexapod robots has been considered from a different point of view. The notion of a locked joint failure is introduced and its effect on robot walking is analyzed based on manipulator kinematics and gait study. A locked joint failure does not reduce stability of a gait but constrain the workspace of the failed leg to a restricted area. We have shown that there is a range of kinematic constraint on the configuration of the failed leg which guarantees the existence of post-failure walking on the straight-line and crab-walking trajectory, respectively. A strategy of fault tolerance for a locked joint failure has been proposed for the hexapod robot, in which the hexapod has discontinuous movement of the body with respect to leg swing and the failed leg is swung passively by the translation of the body. As a special form of the proposed strategy, periodic quadruped and tripod gaits have been proposed for straight-line motion and crab walking, respectively, and their behavior and efficiency have been investigated. By taking the proposed periodic gait, the hexapod can overcome any fault event caused by a locked joint failure and maintain static stability. The transition procedure from the standard wave gait to the proposed periodic gait has been shown as an example to demonstrate the applicability of the proposed scheme.

As further researches, there are fault-tolerant gait planning for irregular gaits on uneven terrain and fault-tolerant gaits considering dynamic effects.

8. References

Chu, K. K. & Pang, K. H. (2002). Comparison between different model of hexapod robot in fault tolerant gait, *IEEE Transactions on Systems, Man, and Cybernetics A*, Vol. 32, No. 6, pp. 752-756.

Craig, J. J. (2003). Introduction to Robotics: Mechanics and Control(3rd Ed.), Prentice Hall, ISBN 0201543613, Upper Saddle River, NJ.

Lee, T. T.; Liao, C. M. & Chen, T. K. (1988). On the stability properties of hexapod tripod gait, *IEEE Transactions on Robotics and Automation*, Vol. 4, No. 4, pp. 427–434.

Lee, Y. J. & Hirose, S. (2002). Three-legged walking for fault-tolerant locomotion of demining quadruped robots, *Advanced Robotics*, Vol. 16, No. 5, pp. 415-426.

Lewis, C. L. & Maciejewski, A. A. (1997). Fault tolerant operation of kinematically redundant manipulators for locked joint failures, *IEEE Transactions on Robotics and Automation*, Vol. 13, No. 4, pp. 622–629.

Lewis, F. L.; Abdallah, C. T. & Dawson, D. M. (1993). *Control of Robot Manipulators*, Macmillan, ISBN 0-02-370501-9, New York.

Miao, S. & Howard, D. (2000). Optimal tripod gait generation for hexapod walking machines, *Robotica*, Vol. 18, No. 6, pp. 639–649.

Nagy, P. V.; Desa, S. & Whittaker, W. L. (1994). Energy based stability measures for reliable locomotion of statically stable walkers: theory and application, *International Journal of Robotics Research*, Vol. 3, No. 3, pp. 272–287.

Roberts, R. G. & Maciejewski, A. A. (1996). A local measure of fault tolerance for kinematically redundant manipulators, *IEEE Transactions on Robotics and Automation*, Vol. 12, No. 4, pp. 543–552.

Shin, J. H. & Lee, J. J. (1999). Fault detection and robust fault recovery control for robot manipulators with actuator failures, *Proceedings of IEEE International Conference on Robotics and Automation*, pp. 861-866, 1999.

Song, S. M. & Choi, B. S. (199). The optimally stable ranges of 2*n*-legged wave gaits, *IEEE Transactions on Systems, Man, and Cybernetics*, Vol. 20, No. 4, pp. 888–902.

Song, S. M. & Waldron, K. J. (1987). An analytical approach for gait study and its application on wave gaits, *International Journal of Robotics Research*, Vol. 6, No. 2, pp. 60-70.

Yang, J. M. & Kim, J. H. (1998). Fault-tolerant locomotion of the hexapod robot, *IEEE Transactions on Systems, Man, and Cybernetics B*, Vol. 28, No. 1, pp. 109–116.

Yang, J. M. (1999). *Fault Tolerant Gaits of Legged Robots*, Ph.D. Dissertation, Korea Advance Institute of Science and Technology, Daejeon, Korea.

Yang, J. M. (2002). Fault tolerant gaits of quadruped robots for locked joint failures, *IEEE Transactions on Systems, Man, and Cybernetics C*, Vol. 32, No. 4, pp. 507-516.

Yang, J. M. (2003). Crab walking of quadruped robots with a locked joint failure, *Advanced Robotics*, Vol. 17, No. 9, pp. 863–878.

Mobile Robotics, Moving Intelligence

Edited by Jonas Buchli

ISBN 3-86611-284-X

Hard cover, 586 pages

Publisher Pro Literatur Verlag, Germany / ARS, Austria

Published online 01, December, 2006

Published in print edition December, 2006

This book covers many aspects of the exciting research in mobile robotics. It deals with different aspects of the control problem, especially also under uncertainty and faults. Mechanical design issues are discussed along with new sensor and actuator concepts. Games like soccer are a good example which comprise many of the aforementioned challenges in a single comprehensive and in the same time entertaining framework. Thus, the book comprises contributions dealing with aspects of the Robotcup competition. The reader will get a feel how the problems cover virtually all engineering disciplines ranging from theoretical research to very application specific work. In addition interesting problems for physics and mathematics arises out of such research. We hope this book will be an inspiring source of knowledge and ideas, stimulating further research in this exciting field. The promises and possible benefits of such efforts are manifold, they range from new transportation systems, intelligent cars to flexible assistants in factories and construction sites, over service robot which assist and support us in daily live, all the way to the possibility for efficient help for impaired and advances in prosthetics.

InTech Europe

University Campus STeP Ri
Slavka Krautzeka 83/A
51000 Rijeka, Croatia
Phone: +385 (51) 770 447
Fax: +385 (51) 686 166
www.intechopen.com

InTech China

Unit 405, Office Block, Hotel Equatorial Shanghai
No.65, Yan An Road (West), Shanghai, 200040, China
中国上海市延安西路65号上海国际贵都大饭店办公楼405单元
Phone: +86-21-62489820
Fax: +86-21-62489821

IntechOpen